Bearing Capacity Prediction of Spatially Random $c - \phi$ Soils

Canadian Geotechnical Journal, 40(1), 54–65, Feb 2003

Gordon A. Fenton
Dalhousie University, Halifax, NS B3J 2X4
Gordon.Fenton@dal.ca
D. V. Griffiths
Colorado School of Mines, Golden, CO 80401
D.V.Griffiths@mines.edu

Abstract

Soils with spatially varying shear strengths are modeled using random field theory and elasto-plastic finite element analysis to evaluate the extent to which spatial variability and cross-correlation in soil properties (c and ϕ) affect bearing capacity. The analysis is two dimensional, corresponding to a strip footing with infinite correlation length in the out-of-plane direction, and the soil is assumed to be weightless with footing placed on the soil surface. Theoretical predictions of the mean and standard deviation of bearing capacity, for the case where c and ϕ are independent, are derived using a geometric averaging model and then verified via Monte Carlo simulation. The standard deviation prediction is found to be quite accurate, while the mean prediction is found to require some additional semi-empirical adjustment to give accurate results for 'worst case' correlation lengths. Combined, the theory can be used to estimate the probability of bearing capacity failure, but also sheds light on the stochastic behaviour of foundation bearing failure.

1. Introduction

The design of a footing involves two limit states; a serviceability limit state, which generally translates into a maximum settlement or differential settlement, and an ultimate limit state. The latter is concerned with the maximum load which can be placed on the footing just prior to a bearing capacity failure. This paper looks at the ultimate bearing capacity of a smooth strip footing founded on a soil having spatially random properties.

Most modern bearing capacity predictions involve a relationship of the form (Terzaghi, 1943)

$$q_f = cN_c + \bar{q}N_q + \tfrac{1}{2}\gamma B N_\gamma \qquad [1]$$

where q_f is the ultimate bearing stress, c is the cohesion, $\bar{q}$ is the overburden stress, γ is the unit soil weight, B is the footing width, and N_c, N_q, and N_γ are the bearing capacity factors. To simplify the analysis in this paper, and to concentrate on the stochastic behaviour of the most important term (at least as far as spatial variation is concerned), the soil is assumed weightless. Under this assumption, the bearing capacity equation simplifies to

$$q_f = cN_c \qquad [2]$$

Bearing capacity predictions, involving specification of the N factors, are often based on plasticity theory (see, e.g., Prandtl, 1921, Terzaghi, 1943, and Sokolovski, 1965) of a rigid base punching into a softer material. These theories assume a *homogeneous* soil underlying the footing – that is,

the soil is assumed to have properties which are spatially constant. Under this assumption, most bearing capacity theories (e.g., Prandtl, 1921, and Meyerhof, 1951, 1963) assume that the failure slip surface takes on a logarithmic spiral shape to give

$$N_c = \frac{e^{\pi \tan\phi} \tan^2\left(\frac{\pi}{4} + \frac{\phi}{2}\right) - 1}{\tan\phi} \quad [3]$$

This relationship has been found to give reasonable agreement with test results (Bowles, 1996) under ideal conditions. In practice, however, it is well known that the actual failure conditions will be somewhat more complicated than a simple logarithmic spiral. Due to spatial variation in soil properties the failure surface under the footing will follow the weakest path through the soil, constrained by the stress field. For example, Figure 1 illustrates the bearing failure of a realistic soil with spatially varying properties. It can be seen that the failure surface only approximately follows a log-spiral on the right side and is certainly not symmetric. In this plot lighter regions represent stronger soil and darker regions indicate weaker soil. The weak (dark) region near the ground surface to the right of the footing has triggered a non-symmetric failure mechanism that is typically at a lower bearing load than predicted by traditional homogeneous and symmetric failure analysis.

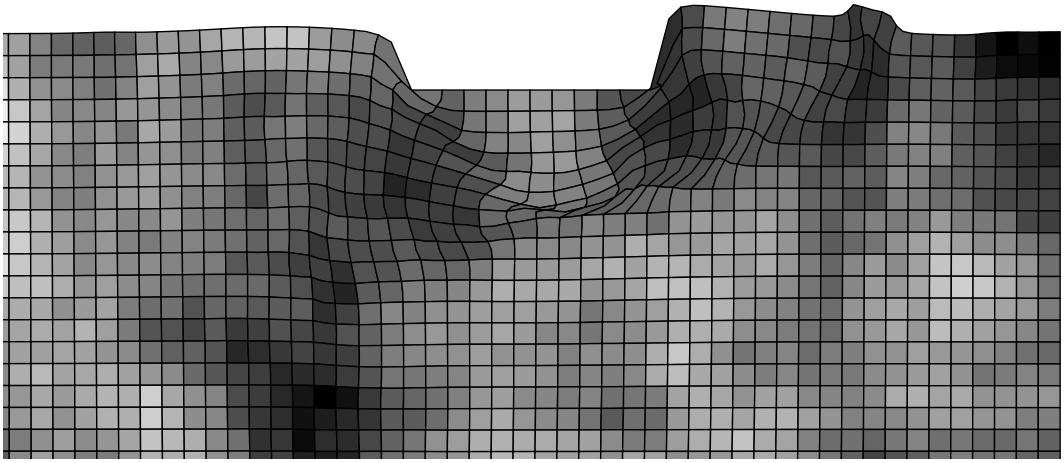

Figure 1. Typical deformed mesh at failure, where the darker regions indicate weaker soil.

The problem of finding the minimum strength failure slip surface through a soil mass is very similar in nature to the slope stability problem, and one which currently lacks a closed form stochastic solution, so far as the authors are aware. In this paper the traditional relationships shown above will be used as a starting point to this problem.

For a realistic soil, both c and ϕ are random, so that both quantities in the right hand side of Eq. (2) are random. This equation can be non-dimensionalized by dividing through by the cohesion mean,

$$M_c = \frac{q_f}{\mu_c} = \frac{c}{\mu_c} N_c \quad [4]$$

where μ_c is the mean cohesion and M_c is the stochastic equivalent of N_c, ie., $q_f = \mu_c M_c$. The stochastic problem is now boiled down to finding the distribution of M_c. A theoretical model for the first two moments (mean and variance) of M_c, based on geometric averaging, are given in the

next section. Monte Carlo simulations are then performed to assess the quality of the predictions and determine the approximate form of the distribution of M_c. This is followed by an example illustrating how the results can be used to compute the probability of a bearing capacity failure. Finally, an overview of the results is given, including their limitations.

2. The Random Soil Model

In this study, the soil cohesion, c, is assumed to be lognormally distributed with mean μ_c, standard deviation σ_c, and spatial correlation length $\theta_{\ln c}$. The lognormal distribution is selected because it is commonly used to represent non-negative soil properties and since it has a simple relationship with the normal. A lognormally distributed random field is obtained from a normally distributed random field, $G_{\ln c}(\underset{\sim}{x})$, having zero mean, unit variance, and spatial correlation length $\theta_{\ln c}$ through the transformation

$$c(\underset{\sim}{x}) = \exp\{\mu_{\ln c} + \sigma_{\ln c} G_{\ln c}(\underset{\sim}{x})\} \tag{5}$$

where $\underset{\sim}{x}$ is the spatial position at which c is desired. The parameters $\mu_{\ln c}$ and $\sigma_{\ln c}$ are obtained from the specified cohesion mean and variance using the lognormal distribution transformations,

$$\sigma^2_{\ln c} = \ln\left(1 + \frac{\sigma_c^2}{\mu_c^2}\right) \tag{6a}$$

$$\mu_{\ln c} = \ln \mu_c - \tfrac{1}{2}\sigma^2_{\ln c} \tag{6b}$$

The correlation coefficient between the log-cohesion at a point $\underset{\sim}{x}_1$ and a second point $\underset{\sim}{x}_2$ is specified by a correlation function, $\rho_{\ln c}(\tau)$, where $\tau = |\underset{\sim}{x}_1 - \underset{\sim}{x}_2|$ is the absolute distance between the two points. In this paper, a simple exponentially decaying (Markovian) correlation function will be assumed, having the form

$$\rho_{\ln c}(\tau) = \exp\left(-\frac{2|\tau|}{\theta_{\ln c}}\right) \tag{7}$$

The spatial correlation length, $\theta_{\ln c}$, is loosely defined as the separation distance within which two values of $\ln c$ are significantly correlated. Mathematically, $\theta_{\ln c}$ is defined as the area under the correlation function, $\rho_{\ln c}(\tau)$ (Vanmarcke, 1984). (Note that geostatisticians often define the correlation length as the area under the non-negative half of the correlation function so that there is a factor of two difference between the two lengths – under their definition, the factor of 2 appearing in Eq. (7) is absent. The more general definition is retained here since it can be used also in higher dimensions where the correlation function is not necessarily symmetric in all directions about the origin.)

It should also be noted that the correlation function selected above acts between values of $\ln c$. This is because $\ln c$ is normally distributed and a normally distributed random field is simply defined by its mean and covariance structure. In practice, the correlation length $\theta_{\ln c}$ can be estimated by evaluating spatial statistics of the log-cohesion data directly (see, e.g., Fenton, 1999). Unfortunately, such studies are scarce so that little is currently known about the spatial correlation

structure of natural soils. For the problem considered here, it turns out that a worst case correlation length exists which should be assumed in the absence of improved information.

The random field is also assumed here to be statistically isotropic (the same correlation length in any direction through the soil). Although the horizontal correlation length is often greater than the vertical, due to soil layering, taking this into account was deemed to be a refinement beyond the scope of this study. The main aspects of the stochastic behaviour of bearing capacity needs to be understood for the simplest case first and more complex variations on the theme, such as site specific anisotropy, left for later work.

The friction angle, ϕ, is assumed to be bounded both above and below, so that neither normal nor lognormal distributions are appropriate. A beta distribution is often used for bounded random variables. Unfortunately, a beta distributed random field has a very complex joint distribution and simulation is cumbersome and numerically difficult. To keep things simple, a bounded distribution is selected which resembles a beta distribution but which arises as a simple transformation of a standard normal random field, $G_\phi(\underset{\sim}{x})$, according to

$$\phi(\underset{\sim}{x}) = \phi_{min} + \tfrac{1}{2}(\phi_{max} - \phi_{min}) \left\{ 1 + \tanh\left(\frac{s G_\phi(\underset{\sim}{x})}{2\pi} \right) \right\} \qquad [8]$$

where ϕ_{min} and ϕ_{max} are the minimum and maximum friction angles, respectively, and s is a scale factor which governs the friction angle variability between its two bounds. Figure 2 shows how the distribution of ϕ (normalized to the interval $[0, 1]$) changes as s changes, going from an almost uniform distribution at $s = 5$ to a very normal looking distribution for smaller s. In all cases, the distribution is symmetric so that the midpoint between ϕ_{min} and ϕ_{max} is the mean. Values of s greater than about 5 lead to a U-shaped distribution (higher at the boundaries), which is not deemed realistic. Thus, varying s between about 0.1 and 5.0 leads to a wide range in the stochastic behaviour of ϕ.

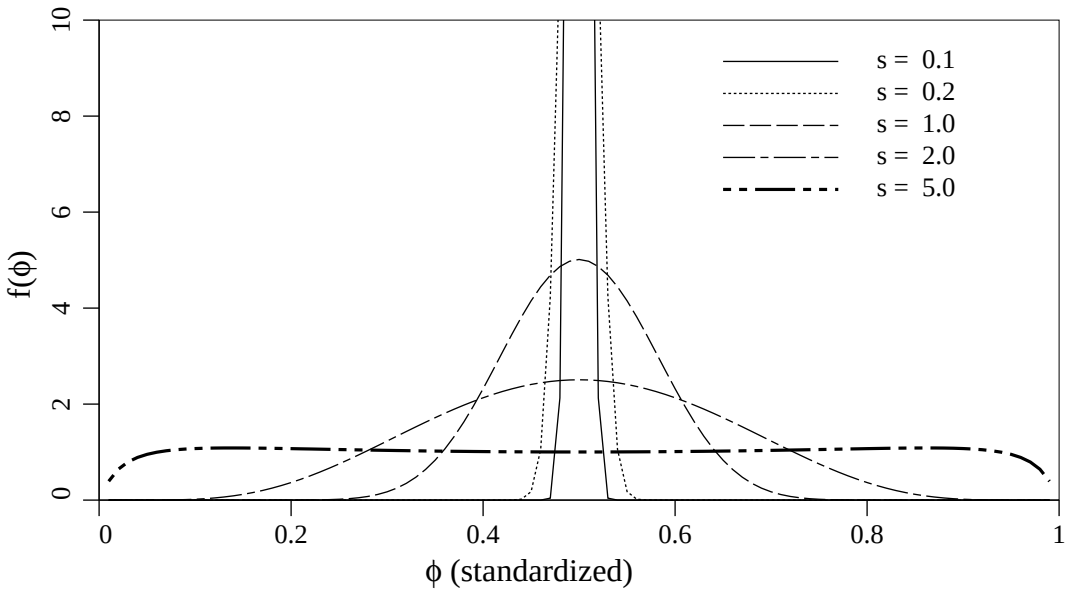

Figure 2. Bounded distribution of friction angle normalized to the interval $[0, 1]$.

The random field, $G_\phi(\underset{\sim}{x})$, has zero mean and unit variance, as does $G_{\ln c}(\underset{\sim}{x})$. Conceivably, $G_\phi(\underset{\sim}{x})$ could also have its own correlation length θ_ϕ distinct from $\theta_{\ln c}$. However, it seems reasonable to

assume that if the spatial correlation structure is caused by changes in the constitutive nature of the soil over space, then both cohesion and friction angle would have similar correlation lengths. Thus, θ_ϕ is taken to be equal to $\theta_{\ln c}$ in this study. Both lengths will be referred to generically from now on simply as θ, remembering that this length reflects correlation between points in the underlying normally distributed random fields, $G_{\ln c}(\underset{\sim}{x})$ and $G_\phi(\underset{\sim}{x})$, and not directly between points in the cohesion and friction fields. As mentioned above, both lengths can be estimated from data sets obtained over some spatial domain by statistically analyzing the suitably transformed data (inverses of Eq's 5 and 8). After transforming to the c and ϕ fields, the transformed correlation lengths will no longer be the same, but since both transformations are monotonic (ie. larger values of $G_{\ln c}$ give larger values of c, etc.), the correlation lengths will be similar (for s = C.O.V. = 1.0, the difference is less than 15% from each other and from the original correlation length). In that all engineering soil properties are derived through various transformations of the physical soil behaviour (eg. cohesion is a complex function of electrostatic forces between soil particles), the final correlation lengths between engineering properties cannot be expected to be identical, only similar. For the purposes of a generic non-site specific study, the above assumptions are believed reasonable.

The question as to whether the two parameters c and ϕ are correlated is still not clearly decided in the literature, and no doubt depends very much on the soil being studied. Cherubini (2000) quotes values of ρ ranging from -0.24 to -0.70, as does Wolff (1985) (see also Yuceman et al., 1973, Lumb, 1970, and Cherubini, 1997). As Wolff says (private correspondence, 2000),

> *The practical meaning of this [negative correlation] is that we are more certain of the undrained strength at a certain confining pressure than the values of the two parameters we use to define it.*

This observation arises from the fact that the variance of the shear strength is reduced if there is a negative correlation between c and ϕ.

In that the correlation between c and ϕ is not certain, this paper investigates the correlation extremes to determine if cross-correlation makes a significant difference. As will be seen, under the given assumptions regarding the distributions of c (lognormal) and ϕ (bounded), varying the cross-correlation ρ from -1 to +1 was found to have only a minor influence on the stochastic behaviour of the bearing capacity.

3. Bearing Capacity Mean and Variance

The determination of the first two moments of the bearing capacity (mean and variance) requires first a failure model. Equations 2 and 3 assume that the soil properties are spatially uniform. When the soil properties are spatially varying, the slip surface no longer follows a smooth log-spiral and the failure becomes unsymmetric. The problem of finding the constrained path having the lowest total shear strength through the soil is mathematically difficult, especially since the constraints are supplied by the stress field. A simpler approximate model will be considered here wherein geometric averages of c and ϕ, over some region under the footing, are used in Equations 2 and 3. The geometric average is proposed because it is dominated more by low strengths than is the arithmetic average. This is deemed reasonable since the failure slip surface preferentially travels through lower strength areas.

Consider a soil region of some size D discretized into a sequence of non-overlapping rectangles, each centered on $\underset{\sim}{x}_i$, $i = 1, 2, \ldots, n$. The geometric average of the cohesion, c, over the domain D may then be defined as

$$[9] \qquad \bar{c} = \left[\prod_{i=1}^{n} c(\underset{\sim}{x}_i)\right]^{1/n} = \exp\left\{\frac{1}{n}\sum_{i=1}^{n} \ln c(\underset{\sim}{x}_i)\right\}$$
$$= \exp\left\{\mu_{\ln c} + \sigma_{\ln c}\bar{G}_{\ln c}\right\}$$

where $\bar{G}_{\ln c}$ is the *arithmetic* average of $G_{\ln c}$ over the domain D. Note that an assumption is made in the above concerning $c(\underset{\sim}{x}_i)$ being constant over each rectangle. In that cohesion is generally measured using some representative volume (eg. a lab sample), the values of $c(\underset{\sim}{x}_i)$ used above are deemed to be such measures.

In a similar way, the exact expression for the geometric average of ϕ over the domain D is

$$[10] \qquad \bar{\phi} = \exp\left\{\frac{1}{n}\sum_{i=1}^{n} \ln \phi(\underset{\sim}{x}_i)\right\}$$

where $\phi(\underset{\sim}{x}_i)$ is evaluated using Eq. (8). A close approximation to the above geometric average, accurate for $s \leq 2.0$, is

$$[11] \qquad \bar{\phi} \simeq \phi_{min} + \tfrac{1}{2}(\phi_{max} - \phi_{min})\left\{1 + \tanh\left(\frac{s\bar{G}_{\phi}}{2\pi}\right)\right\}$$

where $\bar{G}_{\phi}$ is the *arithmetic* average of G_{ϕ} over the domain D. For $\phi_{min} = 5^o$, $\phi_{max} = 45^o$, this expression has relative error of less than 5% for $n = 20$ independent samples. While the relative error rises to about 12%, on average, for $s = 5.0$, this is an extreme case, corresponding to a uniformly distributed ϕ between the minimum and maximum values, which is felt to be unlikely to occur very often in practice. Thus, the above approximation is believed reasonable in most cases.

Using the latter result in Eq. (3) gives the 'effective' value of N_c, $\bar{N}_c$, where the log-spiral model is assumed to be valid using a geometric average of soil properties within the failed region,

$$[12] \qquad \bar{N}_c = \frac{e^{\pi \tan \bar{\phi}} \tan^2\left(\frac{\pi}{4} + \frac{\bar{\phi}}{2}\right) - 1}{\tan \phi}$$

so that, now

$$[13] \qquad M_c = \frac{\bar{c}}{\mu_c}\bar{N}_c$$

If c is lognormally distributed, an inspection of Eq. (9) indicates that $\bar{c}$ is also lognormally distributed. If we can assume that $\bar{N}_c$ is at least approximately lognormally distributed, then M_c will also be at least approximately lognormally distributed (the Central Limit Theorem helps out somewhat here). In this case, taking logarithms of Eq. (13) gives

$$[14] \qquad \ln M_c = \ln \bar{c} + \ln \bar{N}_c - \ln \mu_c$$

so that, under the given assumptions, $\ln M_c$ is at least approximately normally distributed.

The task now is to find the mean and variance of $\ln M_c$. The mean is obtained by taking expectations of Eq. (14),

[15] $$\mu_{\ln M_c} = \mu_{\ln \bar{c}} + \mu_{\ln \bar{N}_c} - \ln \mu_c$$

where

[16] $$\begin{aligned} \mu_{\ln \bar{c}} &= \mathrm{E}\left[\mu_{\ln c} + \sigma_{\ln c}\bar{G}_{\ln c}\right] \\ &= \mu_{\ln c} + \sigma_{\ln c}\mathrm{E}\left[\bar{G}_{\ln c}\right] \\ &= \mu_{\ln c} \\ &= \ln \mu_c - \tfrac{1}{2}\ln\left(1 + \frac{\sigma_c^2}{\mu_c^2}\right) \end{aligned}$$

which used the fact that since $\bar{G}_{\ln c}$ is normally distributed, its arithmetic average has the same mean as $G_{\ln c}$, that is $\mathrm{E}\left[\bar{G}_{\ln c}\right] = \mathrm{E}\left[G_{\ln c}\right] = 0$. The above result is as expected since the geometric average of a lognormally distributed random variable preserves the mean of the logarithm of the variable. Also Eq. (6b) was used to express the mean in terms of the prescribed statistics of c.

A second order approximation to the mean of the logarithm of Eq. (12), $\mu_{\ln \bar{N}_c}$, is

[17] $$\mu_{\ln \bar{N}_c} \simeq \ln \bar{N}_c(\mu_{\bar{\phi}}) + \sigma^2_{\bar{\phi}}\left(\frac{d^2 \ln \bar{N}_c}{d\phi^2}\bigg|_{\mu_{\bar{\phi}}}\right)$$

where $\mu_{\bar{\phi}}$ is the mean of the geometric average of ϕ. Since $\bar{G}_\phi$ is an arithmetic average, its mean is equal to the mean of G_ϕ, which is zero. Thus, since the assumed distribution of ϕ is symmetric about its mean, $\mu_{\bar{\phi}} = \mu_\phi$ so that $\ln \bar{N}_c(\mu_{\bar{\phi}}) = \ln N_c(\mu_\phi)$.

A first order approximation to $\sigma^2_{\bar{\phi}}$ is

[18] $$\sigma^2_{\bar{\phi}} = \left[\frac{s}{4\pi}(\phi_{max} - \phi_{min})\sigma_{\bar{G}_\phi}\right]^2$$

where, from local averaging theory (Vanmarcke, 1984), the variance of a local average over the domain D is given by (recalling that G_ϕ is normally distributed with zero mean and unit variance),

[19] $$\sigma^2_{\bar{G}_\phi} = \sigma^2_{G_\phi}\gamma(D) = \gamma(D)$$

where $\gamma(D)$ is the 'variance function' which reflects the amount that the variance is reduced due to local arithmetic averaging. It can be obtained directly from the correlation function (see Appendix I).

The derivative in Eq. (17) is most easily obtained numerically using any reasonably accurate (N_c is quite smooth) approximation to the second derivative. See, for example, Press et. al. (1997). If $\mu_{\bar{\phi}} = \mu_\phi = 25^o = 0.436$ radians (note that in all mathematical expressions, ϕ is assumed to be in radians), then

[20] $$\frac{d^2 \ln \bar{N}_c}{d\phi^2}\bigg|_{\mu_{\bar{\phi}}} = 5.2984 \quad (\mathrm{rad})^{-2}$$

Using these results with $\phi_{max} = 45^o$ and $\phi_{min} = 5^o$ so that $\mu_\phi = 25^o$ gives

[21] $$\mu_{\ln \bar{N}_c} = \ln(20.72) + 0.0164 s^2 \gamma(D)$$

Some comments need to be made about this result: First of all it increases with increasing variability in ϕ (increasing s). It seems doubtful that this increase would occur since increasing variability in ϕ would likely lead to more lower strength paths through the soil mass for moderate θ. Aside from ignoring the weakest path issue, some other sources of error in the above analysis are

1) the geometric average of ϕ given by Eq. (10) actually shows a slight decrease with s (about 12% less, relatively, when $s = 5$). Although the decrease is only slight, it at least is in the direction expected.
2) an error analysis of the second order approximation in Eq. (17) and the first order approximation in Eq. (18) has not been carried out. Given the rather arbitrary nature of the assumed distribution on ϕ, and the fact that this paper is primarily aimed at establishing the approximate stochastic behaviour, such refinements have been left for later work.

In light of these observations, a first order approximation to $\mu_{\ln \bar{N}_c}$ may actually be more accurate. Namely,

[22] $$\mu_{\ln \bar{N}_c} \simeq \ln \bar{N}_c(\mu_{\bar{\phi}}) \simeq \ln N_c(\mu_\phi)$$

Finally, combining Equations (16) and (22) into Eq. (15) gives

[23] $$\mu_{\ln M_c} \simeq \ln N_c(\mu_\phi) - \tfrac{1}{2} \ln \left(1 + \frac{\sigma_c^2}{\mu_c^2}\right)$$

For independent c and ϕ, the variance of $\ln M_c$ is

[24] $$\sigma^2_{\ln M_c} = \sigma^2_{\ln \bar{c}} + \sigma^2_{\ln \bar{N}_c}$$

where

[25] $$\sigma^2_{\ln \bar{c}} = \gamma(D) \sigma^2_{\ln c} = \gamma(D) \ln \left(1 + \frac{\sigma_c^2}{\mu_c^2}\right)$$

and, to first order,

[26] $$\sigma^2_{\ln \bar{N}_c} \simeq \sigma^2_{\bar{\phi}} \left(\frac{d \ln \bar{N}_c}{d\phi}\bigg|_{\mu_{\bar{\phi}}} \right)^2$$

The derivative appearing in Eq. (26), which will be denoted as $\beta(\phi)$, is

[27] $$\beta(\phi) = \frac{d \ln \bar{N}_c}{d\phi} = \frac{d \ln N_c}{d\phi}$$
$$= \frac{bd}{bd^2 - 1} \left[\pi(1 + a^2)d + 1 + d^2 \right] - \frac{1 + a^2}{a}$$

where $a = \tan(\phi)$, $b = e^{\pi a}$, and $d = \tan\left(\frac{\pi}{4} + \frac{\phi}{2}\right)$.

The variance of $\ln M_c$ is thus

[28] $$\sigma^2_{\ln M_c} \simeq \gamma(D) \left\{ \ln \left(1 + \frac{\sigma_c^2}{\mu_c^2}\right) + \left[\left(\frac{s}{4\pi}\right) (\phi_{max} - \phi_{min}) \beta(\mu_\phi) \right]^2 \right\}$$

where ϕ is measured in radians.

4. Monte Carlo Simulation

A finite element computer program was written to compute the bearing capacity of a smooth rigid strip footing (plane strain) founded on a weightless soil with shear strength parameters c and ϕ represented by spatially varying and cross-correlated (point-wise) random fields, as discussed above. The bearing capacity analysis uses an elastic-perfectly plastic stress-strain law with a classical Mohr-Coulomb failure criterion. Plastic stress redistribution is accomplished using a viscoplastic algorithm. The program uses 8-node quadrilateral elements and reduced integration in both the stiffness and stress redistribution parts of the algorithm. The theoretical basis of the method is described more fully in Chapter 6 of the text by Smith and Griffiths (1998). The finite element model incorporates five parameters; Young's modulus (E), Poisson's ratio (ν), dilation angle (ψ), shear strength (c), and friction angle (ϕ). The program allows for random distributions of all five parameters, however in the present study, E, ν and ψ are held constant (at 100000 kN/m^2, 0.3, and 0, respectively) while c and ϕ are randomized. The Young's modulus governs the initial elastic response of the soil, but does not affect bearing capacity. Setting the dilation angle to zero means that there is no plastic dilation during yield of the soil. The finite element mesh consists of 1000 elements, 50 elements wide by 20 elements deep. Each element is a square of side length 0.1m and the strip footing occupies 10 elements, giving it a width of B = 1 m.

The random fields used in this study are generated using the Local Average Subdivision (LAS) method (Fenton, 1994, Fenton and Vanmarcke 1990). Cross-correlation between the two soil property fields (c and ϕ) is implemented via Covariance Matrix Decomposition (Fenton, 1994). The algorithm is given in Appendix II.

In the parametric studies that follow, the mean cohesion (μ_c) and mean friction angle (μ_ϕ) have been held constant at 100 kN/m^2 and 25^o (with ϕ_{min} = 5^o and ϕ_{max} = 45^o), respectively, while the C.O.V. (= σ_c/μ_c), spatial correlation length (θ), and correlation coefficient, ρ, between $G_{\ln c}$ and G_ϕ are varied systematically according to Table 1.

Table 1. Random field parameters used in the study.

θ	=	0.5	1.0	2.0	4.0	8.0	50.
C.O.V.	=	0.1	0.2	0.5	1.0	2.0	5.0
ρ	=	-1.0	0.0	1.0			

It will be noticed that C.O.V.'s up to 5.0 are considered in this study, which is an order of magnitude higher than generally reported in the literature (see, eg. Phoon and Kulhawy, 1999). There are two considerations which complicate the problem of defining typical C.O.V.'s for soils that have not yet been clearly considered in the literature (although Fenton, 1999, does introduce these issues). The first has to do with the level of information known about a site. Prior to any site investigation, there will be plenty of uncertainty about soil properties, and an appropriate C.O.V. comes by using a C.O.V. obtained from regional data over a much larger scale. Such a C.O.V. will typically be much greater than that found when soil properties are estimated over a much smaller scale, such as a specific site. As investigation proceeds at the site of interest, the C.O.V. drops. For example, a single sample at the site will reduce the C.O.V. slightly, but as the investigation intensifies, the C.O.V. drops towards zero, reaching zero when the entire site has been sampled (which, of course, is clearly impractical). The second consideration, which is actually closely tied to the first, has to do with scale. If one were to take soil samples every 10 km over 5000 km (macroscale), one will find that the C.O.V. of those samples will be very large. A C.O.V. of 5.0 would not be unreasonable. Alternatively, suppose one were to concentrate one's attention on a single cubic metre of soil. If

several 50 mm cubed samples were taken and sent to the laboratory, one would expect a fairly small C.O.V. On the other hand, if samples of size 0.1 μm cubed were taken and tested (assuming this was possible), the resulting C.O.V. could be very large since some samples might consist of very hard rock particles, others of water, and others just of air (ie. the sample location falls in a void). In such a situation, a C.O.V. of 5.0 could easily be on the low side. While the last scenario is only conceptual, it does serve to illustrate that C.O.V. is highly dependent on the ratio between sample volume and sampling domain volume. This dependence is certainly pertinent to the study of bearing capacity since it is currently not known at what scale bearing capacity failure operates. Is the weakest path through a soil dependent on property variations at the micro-scale (having large C.O.V.), or does the weakest path 'smear' the small-scale variations and depend primarily on local average properties over, say, laboratory scales (small C.O.V.)? Since laboratory scales are merely convenient for us, it is unlikely that nature has selected that particular scale to accommodate us. From the point of view of reliability estimates, where the failure mechanism might depend on microscale variations for failure initiation, the small C.O.V.'s reported in the literature might very well be dangerously unconservative. Much work is still required to establish the relationship between C.O.V., site investigation intensity, and scale. In the meantime, this paper considers C.O.V.'s over a fairly wide range, since it is entirely possible that the higher values more truly reflect failure variability.

In addition, it is assumed that when the variability in the cohesion is large, the variability in the friction angle will also be large. Under this reasoning, the scale factor, s, used in Eq. (8) is set to $s = \sigma_c/\mu_c$ = C.O.V.. This choice is arbitrary, but results in the friction angle varying from quite narrowly (when C.O.V. = 0.1 and s = 0.1) to very widely (when C.O.V. = 5.0 and s = 5) between its lower and upper bounds, 5^o and 45^o, as illustrated in Figure 2.

For each set of assumed statistical properties given by Table 1, Monte-Carlo simulations have been performed. These involve 1000 realizations of the soil property random fields and the subsequent finite element analysis of bearing capacity. Each realization, therefore, has a different value of the bearing capacity and, after normalization by the *mean* cohesion, a different value of the bearing capacity factor,

$$[29] \qquad M_{c_i} = \frac{q_{f_i}}{\mu_c}, \quad i = 1, 2, \ldots, 1000, \quad \Longrightarrow \quad \hat{\mu}_{\ln M_c} = \frac{1}{1000}\sum_{i=1}^{1000} \ln M_{c_i}$$

where $\hat{\mu}_{\ln M_c}$ is the sample mean of $\ln M_c$ estimated over the ensemble of realizations. Because of the non-linear nature of the analysis, the computations are quite intensive. One run of 1000 realizations typically takes about 2 days on a dedicated 800 MHz Pentium III computer (which, by the time of printing, is likely obsolete). For the 108 cases considered in Table 1, the total single CPU time required is about 220 days (run time varies with the number of iterations required to analyze various realizations).

4.1 Simulation Results

Figure 3(a) shows how the sample mean log-bearing capacity factor, taken as the average over the 1000 realizations of $\ln M_{c_i}$, and referred to as $\hat{\mu}_{\ln M_c}$ in the Figure, varies with correlation length, soil variability, and cross-correlation between c and ϕ. For small soil variability, $\hat{\mu}_{\ln M_c}$ tends towards the deterministic value of ln(20.72) = 3.03, which is found when the soil takes on its mean properties everywhere. For increasing soil variability, the mean bearing capacity factor becomes quite significantly reduced from the traditional case. What this implies from a design standpoint is that the bearing capacity of a spatially variable soil will, on average, be *less* than the Prandtl solution based on the mean values alone. The greatest reduction from the Prandtl solution is observed for perfectly correlated c and ϕ (ρ = +1), the least reduction when c and ϕ are negatively correlated ($\rho = -1$), and the independent case (ρ = 0) lies between these two extremes. However, the effect of cross-correlation is seen to be not particularly large. If the negative cross-correlation indicated by both Cherubini (2000) and Wolff (1985) is correct, then the independent, ρ = 0, case is conservative, having mean bearing capacities consistently somewhat less than the $\rho = -1$ case.

The cross-correlation between c and ϕ is seen to have minimal effect on the sample standard deviation, $\hat{\sigma}_{\ln M_c}$, as shown in Figure 3(b). The sample standard deviation is most strongly affected by the correlation length and somewhat less so by the soil property variability. A decreasing correlation length results in a decreasing $\hat{\sigma}_{\ln M_c}$. As suggested by Eq. (28), the function $\gamma(D)$ decays approximately with θ/D and so decreases with decreasing θ. This means that $\hat{\sigma}_{\ln M_c}$ should decrease as the correlation length decreases, which is as seen in Figure 3(b).

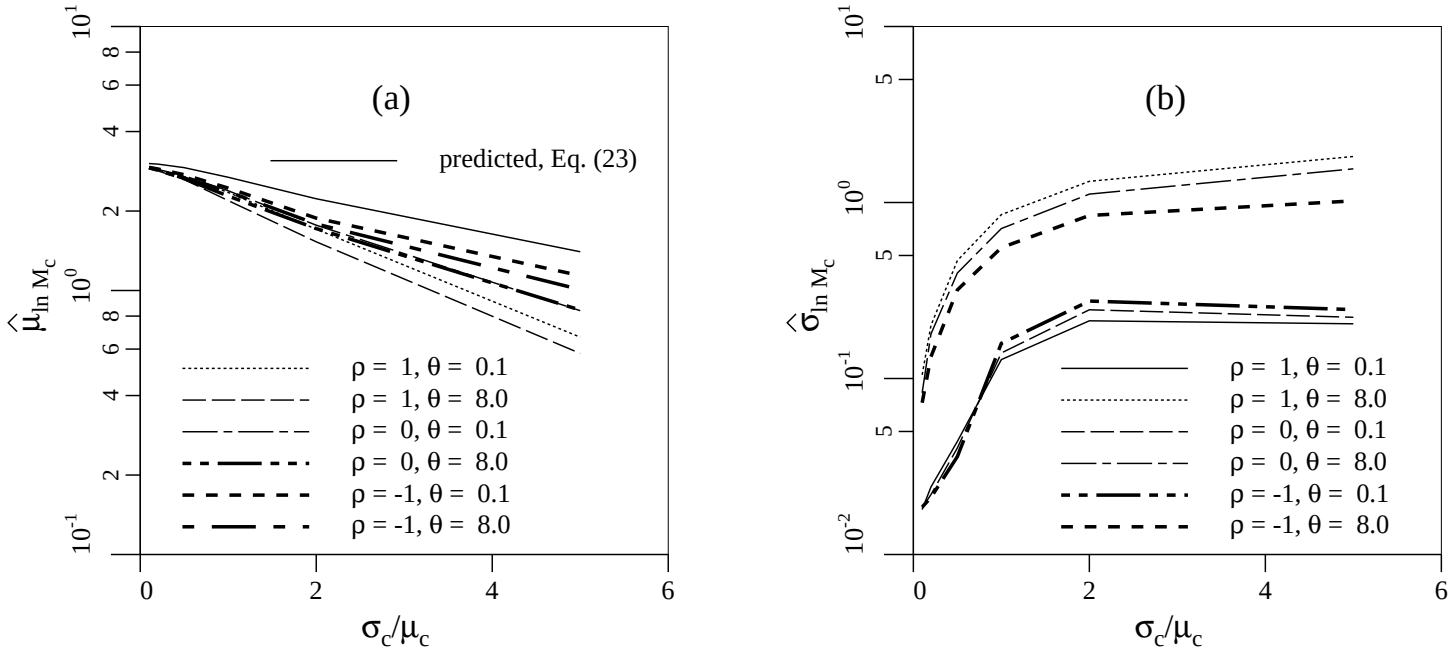

Figure 3. a) Sample mean of log-bearing capacity factor, $\ln M_c$, and b) its sample standard deviation.

Figure 3(a) also seems to show that the correlation length, θ, does not have a significant influence in that the θ = 0.1 and θ = 8 curves for ρ = 0 are virtually identical. However, the θ = 0.1 and θ = 8 curves are significantly lower than that predicted by Eq. (23) implying that the plot is somewhat misleading with respect to the dependence on θ. For example, when the correlation

length goes to infinity, the soil properties become spatially constant, albeit still random from realization to realization. In this case, because the soil properties are spatially constant, the weakest path returns to the log-spiral and $\mu_{\ln M_c}$ will rise towards that given by Eq. (23), namely $\mu_{\ln M_c} = \ln(20.72) - \frac{1}{2}\ln(1 + \sigma_c^2/\mu_c^2)$, which is also shown on the plot. This limiting value holds because $\mu_{\ln N_c} \simeq \ln N_c(\mu_\phi)$, as discussed for Eq. (22), where for spatially constant properties $\bar{\phi} = \phi$.

Similarly, when $\theta \to 0$, the soil property field becomes infinitely "rough", in that all points in the field become independent. Any point at which the soil is weak will be surrounded by points where the soil is strong. A path through the weakest points in the soil might have very low average strength, but at the same time will become infinitely tortuous and thus infinitely long. This, combined with shear interlocking dictated by the stress field, implies that the weakest path should return to the traditional log-spiral with average shear strength along the spiral given by μ_ϕ and the median of c which is $\exp\{\mu_{\ln c}\}$. Again, in this case, $\mu_{\ln M_c}$ should rise to that given by Eq. (23).

The variation of $\mu_{\ln M_c}$ with respect to θ is more clearly seen in Figure 4. Over a range of values of σ_c/μ_c, the value of $\mu_{\ln M_c}$ rises towards that predicted by Eq. (23) at both high and low correlation lengths. At intermediate correlation lengths, the weakest path issue is seen to result in $\mu_{\ln M_c}$ being less than that predicted by Eq. (23) (see Figure 3a), the greatest reduction in $\mu_{\ln M_c}$ occurring when θ is of the same order as the footing width, B. It is hypothesized that $\theta \simeq B$ leads to the greatest reduction in $\mu_{\ln M_c}$ because it allows enough spatial variability for a failure surface which deviates somewhat from the log-spiral but which is not too long (as occurs when θ is too small) yet has significantly lower average strength than the $\theta \to \infty$ case. The apparent agreement between the $\theta = 0.1$ and $\theta = 8$ curves in Figure 3(a) is only because they are approximately equispaced on either side of the minimum at $\theta \simeq 1$.

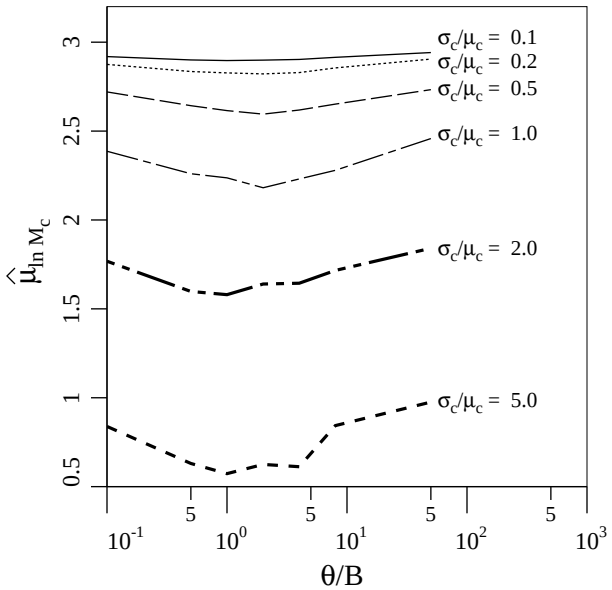

Figure 4. Sample mean of log-bearing capacity factor, $\ln M_c$, versus normalized correlation length.

As noted above, in the case where c and ϕ are independent ($\rho = 0$) the predicted mean, $\mu_{\ln M_c}$, given by Eq. (23) does not decrease as fast as observed in Figure 3(a) for intermediate correlation lengths. Nor does Eq. (23) account for changes in θ. Although an analytic prediction for the mean strength of the constrained weakest path through a spatially random soil has not yet been

determined, Eq. (23) can be improved by making the following empirical corrections for the worst case ($\theta \simeq B$),

[30] $$\mu_{\ln M_c} \simeq 0.92 \ln N_c(\mu_\phi) - 0.7 \ln \left(1 + \frac{\sigma_c^2}{\mu_c^2}\right)$$

where the overall reduction with σ_c/μ_c is assumed to follow the same form as predicted in Eq. (23). Some portion of the above correction may be due to finite element model error (for example, the finite element model slightly underestimates the deterministic value of N_c, giving N_c = 19.6 instead of 20.7, a 2% relative error in $\ln N_c$), but most is attributed to the weakest path issue and model errors arising by relating a spatial geometric average to a failure which is actually taking place along a curve through the 2-D soil mass.

Figure 5 illustrates the agreement between the sample mean of $\ln M_c$ and that predicted by Eq. (30) and between the sample standard deviation of $\ln M_c$ and Eq. (28) for ρ = 0. The estimated mean is seen to be in quite good agreement with the sample mean for all θ when $\sigma_c/\mu_c < 2$, and with the worst case ($\theta = B$) for $\sigma_c/\mu_c > 2$.

The predicted standard deviation was obtained by assuming a geometric average over a region under the footing of depth equal to the mean wedge zone depth,

[31] $$w \simeq \tfrac{1}{2} B \tan\left(\frac{\pi}{4} + \frac{\mu_\phi}{2}\right)$$

and width of about $5w$. This is a rough approximation to the area of the failure region within the mean log-spiral curve on either side of the footing. Thus, D used in the variance function of Eq. (28) is a region of size $5w \times w$.

Although Eq. (23) fails to reflect the effect of θ on the the reduction in the mean log-bearing capacity factor with increasing soil variability, the sample standard deviation is extremely well predicted by Eq. (28) – being only somewhat underpredicted for very small correlation lengths. To some extent the overall agreement in variance is as expected, since the variability along the weakest path will be similar to the variability along any nearby path through a statistically homogeneous medium.

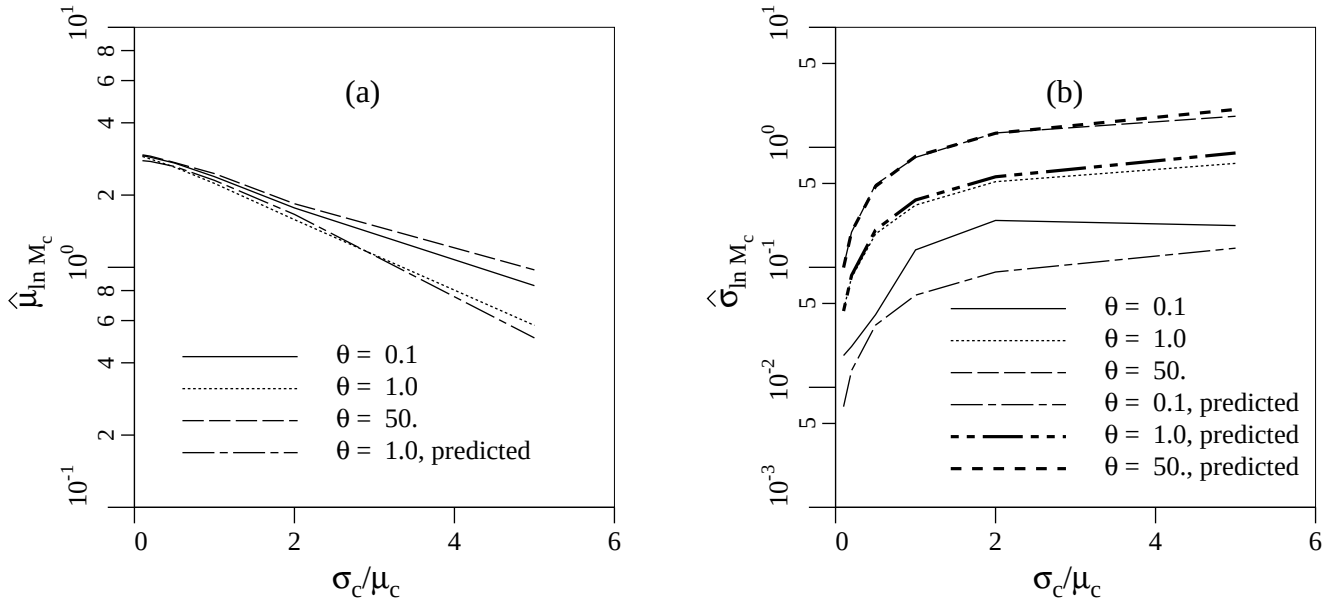

Figure 5. a) Sample and estimated mean (via Eq. 30) of $\ln M_c$, and b) its sample and estimated standard deviation (via Eq. 28).

The Monte Carlo simulation also allows the estimation of the probability density function of M_c. A Chi-Square goodness-of-fit test performed across all σ_c/μ_c, θ, and ρ parameter variations yields an average p-value of 33%. This is encouraging since large p-values indicate good agreement between the hypothesized distribution (lognormal) and the data. However, approximately 30% of the simulations had p-values less than 5%, indicating that a fair proportion of the runs had distributions that deviated from the lognormal to some extent. Some 10% of runs had p-values less than 0.01%. Figure 6(a) illustrates one of the better fits, with a p-value of 43% (σ_c/μ_c = 0.1, θ = 4, and ρ = 0), while Figure 6(b) illustrates one of the poorer fits, with a p-value of 0.01% (σ_c/μ_c = 5, θ = 1, and ρ = 0). It can be seen that even when the p-value is as low as 0.01%, the fit is still reasonable. There was no particular trend in degree of fit as far as the three parameters σ_c/μ_c, θ, and ρ was concerned. It appears, then, that M_c at least approximately follows a lognormal distribution. Note that if M_c does indeed arise from a geometric average of the underlying soil properties, c and N_c, then M_c will tend to a lognormal distribution by the Central Limit Theorem. It is also worth pointing out that this may be exactly why so many soil properties tend to follow a lognormal distribution.

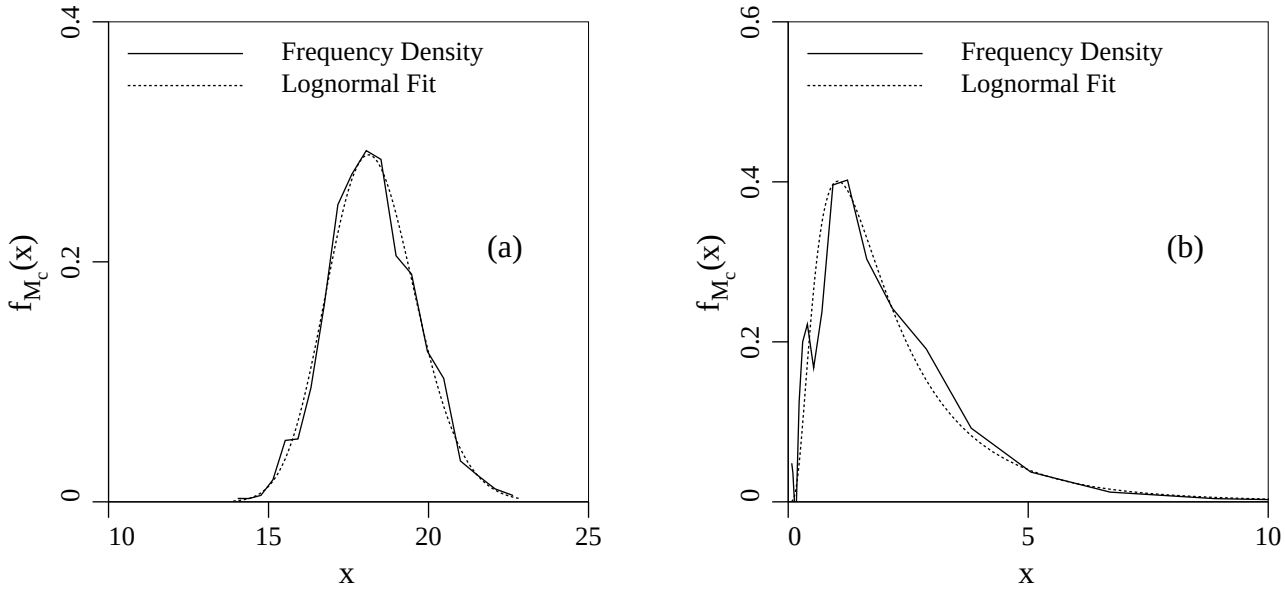

Figure 6. a) Fitted lognormal distribution for $s = \sigma_c/\mu_c$ = 0.1, θ = 4, and ρ = 0 where the p-value is large (0.43) and b) fitted lognormal distribution for $s = \sigma_c/\mu_c$ = 5, θ = 1, and ρ = 0 where the p-value is quite small (0.0001).

5. Probabilistic Interpretation

The results of the previous section indicated that Prandl's bearing capacity formula is still largely applicable in the case of spatially varying soil properties if geometrically averaged soil properties are used in the formula. The theoretical results presented above combined with the empirical correction to the mean proposed in the last section allows the approximate computation of probabilities associated with bearing capacity of a smooth strip footing. To illustrate this, consider an example strip footing of width B = 2 m founded on a weightless soil having μ_c = 75 kPa, σ_c = 50 kPa, and $\theta = B$ = 2 m (assuming the worst case correlation length). Assume also that the friction angle ϕ is

independent of c (conservative assumption) and ranges from 5^o to 35^o, with mean 20^o and $s = 1$. In this case, the deterministic value of N_c, based purely on μ_ϕ is

$$[32] \qquad N_c(\mu_\phi) = \frac{e^{\pi \tan \mu_\phi} \tan^2\left(\frac{\pi}{4} + \frac{\mu_\phi}{2}\right) - 1}{\tan \mu_\phi} = 14.835$$

so that, by Eq. (30),

$$[33] \qquad \mu_{\ln \bar{M}_c} = 0.92 \ln(14.835) - 0.7 \ln\left(1 + \frac{50^2}{75^2}\right) = 2.2238$$

For a footing width of $B = 2$, the wedge zone depth is

$$[34] \qquad w = \tfrac{1}{2} B \tan\left(\frac{\pi}{4} + \frac{\mu_\phi}{2}\right) = \tan\left(\frac{\pi}{4} + \frac{20\pi}{360}\right) = 1.428$$

Averaging over depth w by width $5w$ results in the variance reduction

$$\gamma(D) = \gamma(5w, w) = 0.1987$$

using the algorithm given in Appendix I for the Markov correlation function.

The slope of $\ln N_c$ at $\mu_\phi = 20^o$ is 3.62779 (rad^{-1}), using Eq. (27). These results applied to Eq. (28) give

$$[35] \qquad \sigma^2_{\ln \bar{M}_c} = 0.1987 \left\{ \ln\left(1 + \frac{50^2}{75^2}\right) + \left[\frac{s}{4\pi}(\phi_{max} - \phi_{min})\beta(\mu_\phi\right]^2 \right\} = 0.07762$$

so that $\sigma_{\ln \bar{M}_c} = 0.2778$.

The probability that M_c is less than half the deterministic value of N_c, based on μ_ϕ, is, then

$$[36] \qquad \mathrm{P}\left[M_c \le \frac{14.835}{2}\right] = \Phi\left(\frac{\ln(14.835/2) - \mu_{\ln M_c}}{\sigma_{\ln M_c}}\right) = \Phi(-0.79) = 0.215$$

where Φ is the cumulative distribution function for the standard normal and where M_c is assumed lognormally distributed, as was found to be reasonable above. A simulation of the above problem yields $\mathrm{P}\left[M_c \le \frac{14.835}{2}\right] = 0.2155$. Although this amazing agreement seems too good to be true, this is, in fact, the first example problem that the authors considered. The caveat, however, is that predictions derived from the results of a finite element program are being compared to the results of the same finite element program, albeit at different parameter values. Nevertheless, the fact that the agreement here is so good is encouraging since it indicates that the theoretical results given above may have some overall generality – namely that Prandtl's bearing capacity solution is applicable to spatially variable soils if the soil properties are taken from geometric averages, suitably modified to reflect weakest path issues. Inasmuch as the finite element method represents the actual soil behaviour, this observation seems reasonable.

6. Concluding Remarks

Most soil properties are local averages of some sort and are derived from measurements of properties over some finite volume. In the case of the shear resistance of a soil sample, tests involve determining the average shear resistance over some surface through the soil sample. Since this surface will tend to avoid the high strength areas in favour of low strength areas, the average will be less than a strictly arithmetic mean over a flat plane. Of the various common types of averages – arithmetic, geometric, and harmonic – the one that generally shows the best agreement with 'block' soil properties is the geometric average. The geometric average favours low strength areas, although not as drastically as does a harmonic average, lying between the arithmetic and harmonic averages.

The bearing capacity factor of Prandtl (1921) has been observed in practice to give reasonable agreement with test results, particularly under controlled conditions. When soil properties become spatially random, the failure surface migrates from the log-spiral surface to some nearby surface which is weaker. The results presented in this paper indicate that the statistics of the resulting surface are well represented by geometrically averaging the soil properties over a domain of about the size of the plastically deformed bearing failure region (taken to be $5w \times w$ in this study). That is, that Prandtl's formula can be used to predict the statistics of bearing capacity if the soil properties used in the formula are based on geometric averages, with some empirical adjustment for the mean.

In this sense, the weakest path through the soil is what governs the stochastic bearing capacity behaviour. This means that the details of the distributions selected for c and ϕ are not particularly important, so long as they are physically reasonable, unimodal, and continuous. Although the lognormal distribution, for example, is mathematically convenient when dealing with geometric averages, very similar bearing capacity results are expected using other distributions, such as the normal distribution (suitably truncated to avoid negative strengths). The distribution selected for the friction angle basically resembles a truncated normal distribution over most values of s, but, for example, it is believed that a beta distribution could also have been used here without significantly affecting the results.

In the event that the soil is statistically anisotropic, that is that the correlation lengths differ in the vertical and horizontal directions, it is felt that the above results can still be used with some accuracy by using the algorithm of Appendex I with differing vertical and horizontal correlation lengths. However, some additional study is necessary to establish whether the mean bearing capacity in the anisotropic case is at least conservatively represented by Eq. (30).

Some limitations to this study are noted as follows;

1) The simulations were performed using a finite element analysis in which the values of the underlying normally distributed soil properties assigned to the elements are derived from arithmetic averages of the soil properties over each element domain. While this is believed to be a very realistic approach, intimately related to the soil property measurement process, it is nevertheless an approach where geometric averaging is being performed at the element scale (at least for the cohesion – note that arithmetic averaging of a normally distributed field corresponds to geometric averaging of the associated lognormally distribution random field) in a method which is demonstrating that geometric averaging is applicable over the site scale. Although it is felt that the fine scale averaging assumptions should not significantly affect the large scale results through the finite element method, there is some possibility that there are effects that are not reflected in reality.

2) Model error has been entirely neglected in this analysis. That is, the ability of the finite element method to reflect the actual behaviour of an ideal soil, and the ability of Eq. (3) to do likewise have not been considered. It has been assumed that the finite element method and Eq. (3) are sufficiently reasonable approximations to the behaviour of soils to allow the investigation of the major features of stochastic soil behaviour under loading from a smooth strip footing. Note that the model error associated with traditional usage of Eq. (3) may be due in large part precisely to spatial variation of soil properties, so that this study may effectively be reducing, or at least quantifying, model error (although whether this is really true or not will have to wait until sufficient experimental evidence has been gathered).

The geometric averaging model has been shown to be a reasonable approach to estimating the statistics of bearing capacity. This is particularly true of the standard deviation. Some adjustment was required to the mean, since the geometric average was not able to completely account for the weakest path at intermediate correlation lengths. The proposed relationships for the mean and standard deviation, along with the simulation results indicating that the bearing capacity factor, M_c, is lognormally distributed, allow reasonably accurate calculations of probabilities associated with the bearing capacity. In the event that little is known about the cross-correlation of c and ϕ at a particular site, assuming that these properties are independent is deemed to be conservative (as long as the actual correlation is negative). In any case, the cross-correlation was not found to be a significant factor in the stochastic behaviour of bearing capacity.

Perhaps more importantly, since little is generally known about the correlation length at a site, the results of this study indicate that there exists a worst case correlation length of $\theta \simeq B$. Using this value, in the absence of improved information, allows conservative estimates of the probability of bearing failure. The estimate of the mean log-bearing capacity factor (Eq. 30) is based on this conservative case.

Acknowledgements

The authors would like to thank the National Sciences and Engineering Research Council of Canada, under operating grant OPG0105445, and to the National Science Foundation of the United States of America, under grant CMS-9877189, for their essential support of this research. Any opinions, findings, conclusions or recommendations are those of the authors and do not necessarily reflect the views of the aforementioned organizations.

References

Bowles, J.E. 1996. *Foundation Analysis and Design*, (5th Ed.), McGraw-Hill, New York, NY.

Cherubini, C. 2000. Reliability evaluation of shallow foundation bearing capacity on c', ϕ' soils, *Canadian Geotechnical Journal*, **37**, 264–269.

Cherubini, C. 1997. Data and considerations on the variability of geotechnical properties of soils., *Proceedings of the Int. Conf. on Safety and Reliability (ESREL) 97*, Vol. 2, Lisbon, 1583–1591.

Fenton, G.A. 1994. Error evaluation of three random field generators, *ASCE Journal of Engineering Mechanics*, **120**(12), 2478–2497.

Fenton, G.A. and Vanmarcke, E.H. 1990. Simulation of Random Fields via Local Average Subdivision, *ASCE Journal of Engineering Mechanics*, **116**(8), 1733–1749.

Fenton, G.A. 1999. Estimation for stochastic soil models, *ASCE Journal of Geotechnical and Geoenvironmental Engineering*, **125**(6), 470–485.

Lumb, P. 1970. Safety factors and the probability distribution of soil strength, *Canadian Geotechnical Journal*, **7**, 225–242.

Meyerhof, G. G. 1963. Some recent research on the bearing capacity of foundations, *Canadian Geotechnical Journal*, **1**(1), 16–26.

Meyerhof, G. G. 1951. The ultimate bearing capacity of foundations, *Géotechnique*, **2**(4), 301–332.

Phoon, K-K. and Kulwawy, F.H. 1999. Characterization of geotechnical variability, *Canadian Geotechnical Journal*, **36**, 612–624.

Prandtl, L. 1921. Uber die Eindringungsfestigkeit (Harte) plastischer Baustoffe und die Festigkeit von Schneiden, *Zeitschrift fur angewandte Mathematik und Mechanik*, **1**(1), 15–20.

Press, W.H., Teukolsky, S.A., Vetterling, W.T. and Flannery, B.P. 1997. *Numerical Recipes in C: The Art of Scientific Computing*, ((2nd Ed.)), Cambridge University Press, New York.

Smith, I.M. and Griffiths, D.V. 1998. *Programming the Finite Element Method*, ((3rd Ed.)), John Wiley & Sons, New York, NY.

Sokolovski, V.V. 1965. *Statics of Granular Media*, 270 pages, Pergamon Press, London, UK.

Terzaghi, K. 1943. *Theoretical Soil Mechanics*, John Wiley & Sons, New York, NY.

Vanmarcke, E.H. 1984. *Random Fields: Analysis and Synthesis*, The MIT Press, Cambridge, Massachusetts.

Wolff, T.H. 1985. Analysis and design of embankment dam slopes: a probabilistic approach, Ph.D. Thesis, Purdue University, Lafayette, Indiana.

Yuceman, M.S., Tang, W.H. and Ang, A.H.S. 1973. A probabilistic study of safety and design of earth slopes , Civil Engineering Studies, University of Illinois, Urbana, Structural Research Series 402, Urbana-Champagne, Illinois.

List of Symbols

The following symbols are used in this paper:

a= $\tan\phi$ in Eq. (27)
b= $e^{\pi\tan\phi}$ in Eq. (27)
B= footing width
c= cohesion
$\bar{c}$= geometric average of cohesion field over domain D
d= $\tan(\frac{\pi}{4}+\frac{\phi}{2})$ in Eq. (27)
D= averaging domain ($5w \times w$)
E= elastic modulus
$\mathrm{E}[\cdot]$= expectation operator
$G_1(\underset{\approx}{x})$= standard normal random field
$G_2(\underset{\approx}{x})$= standard normal random field
$G_{\ln c}$= standard normal random field (log-cohesion)
G_ϕ= standard normal random field (underlying friction angle)
$\bar{G}_{\ln c}$= arithmetic average of $G_{\ln c}$ over domain D
$\bar{G}_\phi$= arithmetic average of G_ϕ over domain D
$\underset{\approx}{L}$= lower triangular matrix, square root of covariance matrix
$\tilde{M}_c$= stochastic equivalent of the N_c factor

M_{c_i}= ith realization of M_c
$N_{\underline{c}}$= N-factor associated with cohesion
N_c= cohesion N-factor based on a geometric average of cohesion
N_q= N-factor associated with overburden
N_γ= N-factor associated with the base width and unit weight
$q_{\underline{f}}$= ultimate bearing stress
$\overline{q}$= overburden stress
s= scale factor in distribution of ϕ
$\underset{\sim}{x}$= spatial coordinate, (x_1, x_2) in 2-D
$\underset{\sim}{x}_i$= spatial coordinate of the center of the ith element
$\beta(\phi)$= derivated of N_c, with respect to ϕ, at ϕ
$\underline{\phi}$= friction angle (radians unless otherwise stated)
$\overline{\phi}$= geometric average of ϕ over domain D
ϕ_{min}= minimum friction angle
ϕ_{max}= maximum friction angle
Φ= standard normal cumulative distribution function
$\gamma(D)$= variance function giving variance reduction due to averaging over domain D
μ_c= cohesion mean
$\mu_{\ln c}$= log-cohesion mean
$\mu_{\ln M_c}$= mean of ln M_c
$\hat{\mu}_{\ln M_c}$= sample mean of ln M_c (from simulations)
$\mu_{\ln \overline{\underline{c}}}$= mean of the logarithm of $\overline{\underline{c}}$
$\mu_{\ln \bar{N}_c}$= mean of the logarithm of $\bar{N}_c$
$\mu_{\underline{\phi}}$= mean friction angle
$\mu_{\overline{\phi}}$= mean of $\overline{\phi}$
ν= Poisson's ratio
θ= correlation length of the random fields
$\theta_{\ln c}$= correlation length of the log-cohesion field
θ_ϕ= correlation length of the G_ϕ field
ρ= correlation coefficient
$\rho_{\ln c}(\tau)$= correlation function giving correlation between two points in the log-cohesion field
$\underset{\approx}{\rho}$= correlation matrix
$\underset{\approx}{\sigma}_c$= cohesion standard deviation
$\sigma_{\ln c}$= log-cohesion standard deviation
$\sigma_{\ln \overline{\underline{c}}}$= standard deviation of $\ln \overline{\underline{c}}$
$\sigma_{\overline{\phi}}$= standard deviation of $\overline{\phi}$
σ_{G_ϕ}= standard deviation of $G_{\underline{\phi}}$ (which is 1.0)
$\sigma_{\overline{G}_\phi}$= standard deviation of $\overline{G}_\phi$
$\sigma_{\ln M_c}$= standard deviation of ln M_c
$\hat{\sigma}_{\ln M_c}$= sample standard deviation of ln M_c (from simulations)
τ= distance between two points in the soil domain
ψ= dilation angle

Appendix I

The variance reduction function $\gamma(D)$ gives the amount that the variance of a local average over the domain D is reduced from the point variance. If D is a rectangle of dimension $X \times Y$, then γ is actually a function of X and Y and is defined as

$$[A1] \qquad \gamma(X,Y) = \frac{1}{X^2Y^2}\int_0^X\int_0^X\int_0^Y\int_0^Y \rho(\xi_1-\eta_1,\xi_2-\eta_2)\,d\xi_1\,d\eta_1\,d\xi_1\,d\eta_2$$

where $\rho(\tau_1,\tau_2) = \rho_{\ln c}\left(\sqrt{\tau_1^2+\tau_2^2}\right)$ (see Eq. 7). Since ρ is quandrant symmetric ($\rho(\tau_1,\tau_2) = \rho(-\tau_1,\tau_2) = \rho(\tau_1,-\tau_2) = \rho(-\tau_1,-\tau_2)$), the four-fold integration in Eq. (A1) can be reduced to a two-fold integration,

$$[A2] \qquad \gamma(X,Y) = \frac{4}{X^2Y^2}\int_0^X\int_0^Y (X-\tau_1)(Y-\tau_2)\,\rho(\tau_1,\tau_2)\,d\tau_1\,d\tau_2$$

which can be numerically calculated accurately and efficiently using a 5-point Gauss integration scheme as follows.

$$[A3] \qquad \gamma(X,Y) = \frac{1}{4}\sum_{i=1}^{5} w_i(1-z_i)\sum_{j=1}^{5} w_j(1-z_j)\rho(\xi_i,\eta_j)$$

where

$$\xi_i = \frac{X}{2}(1+z_i)$$
$$\eta_j = \frac{Y}{2}(1+z_j)$$

and the weights, w_i, and Gauss points, z_i, are as follows;

i	w_i	z_i
1	0.236926885056189	-0.906179845938664
2	0.478628670499366	-0.538469310105683
3	0.568888888888889	0.000000000000000
4	0.478628670499366	0.538469310105683
5	0.236926885056189	0.906179845938664

Appendix II

The cross-correlated random c and ϕ fields are obtained via Covariance Matrix Decomposition, as follows;

1) specify the cross-correlation coefficient, ρ ($-1 \leq \rho \leq 1$), from statistical analyses. Three extreme cases are considered in this study: $\rho = -1$, 0 and 1, corresponding to completely negatively correlated, uncorrelated, and completely positively correlated, respectively.

2) form the correlation matrix between $G_{\ln c}(\underset{\sim}{x})$ and $G_{\phi}(\underset{\sim}{x})$, assumed to be stationary, ie. the same at all points $\underset{\sim}{x}$ in the field,

$$\underset{\approx}{\rho} = \begin{bmatrix} 1.0 & \rho \\ \rho & 1.0 \end{bmatrix}$$

3) compute the Cholesky decomposition of $\underset{\approx}{\rho}$. That is, find a lower triangular matrix $\underset{\approx}{L}$ such that $\underset{\approx}{L}\underset{\approx}{L}^T = \underset{\approx}{\rho}$. This is sometimes referred to as the square root of $\underset{\approx}{\rho}$. Note that when $\rho = \pm 1$, $\underset{\approx}{L}$ has the special form

$$\underset{\approx}{L} = \begin{bmatrix} 1.0 & 0.0 \\ \pm 1.0 & 0.0 \end{bmatrix}$$

4) generate two independent standard normally distributed random fields, $G_1(\underset{\sim}{x})$ and $G_2(\underset{\sim}{x})$, each having spatial correlation length θ (see Eq. 7).

5) at each spatial point, $\underset{\sim}{x}_i$, form the underlying point-wise correlated random fields

$$\begin{Bmatrix} G_{\ln c}(\underset{\sim}{x}_i) \\ G_{\phi}(\underset{\sim}{x}_i) \end{Bmatrix} = \begin{bmatrix} L_{11} & 0.0 \\ L_{21} & L_{22} \end{bmatrix} \begin{Bmatrix} G_1(\underset{\sim}{x}_i) \\ G_2(\underset{\sim}{x}_i) \end{Bmatrix}$$

6) use Eq's 5 and 8 to form the final c and ϕ random fields which are then mapped to the finite element mesh to specify the properties of each element.